



Effect of field cooling process and ion-beam bombardment on the exchange bias of NiCo/(Ni, Co)O bilayers



X. Li ^a, K.-W. Lin ^{b,*}, H.-Y. Liu ^b, D.-H. Wei ^c, G.J. Li ^a, P.W.T. Pong ^{a,*}

^a Department of Electrical and Electronic Engineering, The University of Hong Kong, Hong Kong

^b Department of Materials Science and Engineering, National Chung Hsing University, Taichung 402, Taiwan

^c National Synchrotron Radiation Research Center, Hsinchu 300, Taiwan

ARTICLE INFO

Available online 18 March 2014

Keywords:

Magnetic thin films

Exchange bias

Ion-beam bombardment

ABSTRACT

The research on exchange coupled ferromagnetic/antiferromagnetic (FM/AF) bilayers has been the foundation of spintronic applications such as hard disk reading heads and spin torque oscillators. In order to further explore the exchange bias behavior of NiCo/(Ni, Co)O bilayers, effect of field cooling process, magnetic angular dependence, and ion-beam bombardment was investigated. The difference in film composition resulted in remarkable distinction in crystalline structures and domain patterns. The exchange bias field (H_{ex}) in the bilayer systems exhibited a strong angular dependence. The negative H_{ex} after a field cooling process indicated that the polarity of H_{ex} can be defined by aligning the magnetization orientation of the FM NiCo layer with the applied field. Moreover, enhanced exchange bias effect was observed in the NiCo/(Ni, Co)O bilayers that resulted from the surface of the (Ni, Co)O layers bombarded with different Ar^+ ion-beam energies using End-Hall voltages from 0 V to 150 V. The interface spin structures as well as the surface domain patterns were altered by the ion-beam bombardment process. These results indicated that the exchange bias field of NiCo/(Ni, Co)O bilayer systems could be tailored by field cooling process, angular dependence of magnetic properties, and post ion-beam bombardment.

© 2014 Elsevier B.V. All rights reserved.

1. Introduction

Ever since the discovery of exchange anisotropy in Co particles covered with CoO coatings [1], exchange bias has been intensively investigated in both nanostructure composites [2,3] and ferromagnetic/antiferromagnetic (FM/AF) bilayers [4,5]. In the early observations, the center of hysteresis loop of a FM/AF bilayer structure shifted from zero to negative (this shift is known as exchange bias field (H_{ex})) as a result of the exchange coupling in the interface of FM/AF layer [6,7]. However, further research theoretically predicted and experimentally proved the existence of positive exchange bias field in Fe/FeF₂ [8] and Fe/MnF₂ [9] bilayer systems. One possible explanation for such anomalous phenomena attributes the sign of H_{ex} to the coupling mechanism in the AF and FM interface [8,10–14]. As calculated by Koon [15], the orientation of AF spins is perpendicular to the FM axis direction. If the FM and AF couple ferromagnetically (FM coupling), the AF orientation cants towards the FM direction. In the magnetization reversal process, higher negative magnetic field is then required to overcome the coupling between AF and FM layers, resulting in normally negative shift of the hysteresis

loop. On the contrary, AF coupling, where the AF magnetic orientation cants away from FM axis direction, results in positive H_{ex} .

The polarity and magnitude of exchange bias field are influenced by several factors. Firstly, the composition is important in determining the microstructure and thus the magnetic properties of exchange coupled bilayers. Negative H_{ex} was observed in NiFe/FeMn bilayers [16], while NiFe/CoO tends to exhibit positive H_{ex} [5]. Even in the same bilayer system, the difference in AF content would result in dissimilar exchange bias behavior. In our previous research, the content of the oxides was adjusted by changing the O₂/Ar ratio during the preparation of dual ion-beam deposited NiFe/(Ni, Fe)O [17] and NiCo/(Ni, Co)O [18] bilayers. The exchange bias field of both bilayers exhibited strong reliance on the composition of AF layer.

Secondly, when the bilayer structures are cooled through the Neel temperature (T_N) of the AF layer, the cooling field effect also influences the sign of H_{ex} to a great extent. In NiFe/(Ni, Fe)O bilayers, cooling down with no applied field constituted positive H_{ex} , whereas cooling down with a positive cooling field formed negative H_{ex} [11]. On the other hand, many structures exhibited a shift from negative H_{ex} to positive H_{ex} with increasing cooling field, such as (1) ferromagnetic/ferrimagnetic transition-metal rare-earth alloy thin films (CoNi/Gd/CoNi trilayers and CoNi/Gd bilayers [13]), (2) ferrimagnetic/ferrimagnetic bilayers (GdFe/TbFe [19]), (3) ferrimagnetic/ferromagnetic bilayers (FeGd/FeSn [20]), and (4) certain FM/AF bilayers (such as Fe/FeF₂ [8], Fe/MnF₂ [9], GdFe/

* Corresponding authors.

E-mail addresses: kwlin@dragon.nchu.edu.tw (K.-W. Lin), ppong@eee.hku.hk (P.W.T. Pong).

NiCoO [12] and Fe/MnF₂ [14]). When these bilayers are cooled in magnetic field, the orientation of the AF interface spins is influenced by the competition between the interface exchange coupling and the external magnetic force. Under small cooling field, the AF spin configuration is dominated by the interface coupling. However, when the cooling field is so high that the Zeeman energy of the AF interfacial spins is comparable to that of the exchange coupling unidirectional anisotropy energy, the orientation of AF spins is aligned towards the direction of the external field [21]. When the competition between the external magnetic field and the internal unidirectional anisotropy energy reaches a balance, the loop shift can be expressed by the following equation [22]:

$$H_{ex} = \frac{\Delta\sigma}{2\mu_0 M_{FM} t_{FM}} \quad (1)$$

where M_{FM} and t_{FM} are the saturation magnetization and thickness of the ferromagnetic layer, respectively, while $\Delta\sigma$ is the change of the interfacial exchange energy density upon the reversal of the magnetization of the FM layer.

Thirdly, ion bombardment is effective in altering the surface status and domain alignments of magnetic materials [18,23–27]. Ion-beam bombardment can be conducted during the deposition of a certain layer, or after the deposition as a post-treatment. During the ion-bombardment process, the factors that govern the magnetic properties of thin films, including chemical composition, crystallinity, grain sizes and their distribution, can be altered [24]. The research on ion-beam bombarded NiFe/NiO bilayers indicated that by varying the bombardment energies and durations, the NiO spin structures could be modified and the coupling type could be changed [27]. As such, the exchange bias can be tailored by ion-beam bombardment.

Ni and Co are two commonly used FM materials. Their oxides are AF with high Neel temperature ($T_N(\text{CoO}) = 293 \text{ K}$, $T_N(\text{NiO}) = 525 \text{ K}$ [6]). In our previous research, the field cooling effect [26,28] and post ion-beam bombardment effect [23] on the magnetic properties of NiFe/(Ni, Fe)O bilayers were systematically investigated. Our preliminary work revealed that the magnetic properties of NiCo/(Ni, Co)O bilayers were strongly influenced by the O₂/Ar ratio and bombardment voltage of the assisting ion source during the in-situ oxidization of NiCo [18]. In this paper, we further investigate the influence of field cooling process, angular dependence of magnetic properties and post ion-beam bombardment on the microstructure as well as the magnetic behavior of such bilayers.

2. Experimental details

NiCo (10 nm)/(Ni, Co)O (25 nm) bilayers were prepared by dual-ion-beam deposition technique, as described previously [17,23,29]. A Kaufman deposition source ($V_K = 800 \text{ V}$) was engaged to sputter the Ni₅₀Co₅₀ target. The bottom (Ni, Co)O layers were prepared by in-situ oxidization under different O₂/Ar ratios of 0%, 8%, 26% and 30% with an End-Hall assisting source operating at End Hall voltage (V_{EH}) of 100 V. The top NiCo layers were subsequently deposited onto the (Ni, Co)O layers directly or after the ion-beam bombardment process. The base pressure of the chamber was $5.3 \times 10^{-5} \text{ Pa}$ before the deposition process while the coating pressure was around $6.7 \times 10^{-2} \text{ Pa}$.

In order to investigate the field cooling effect, NiCo/(Ni, Co)O (8% O₂/Ar and 30% O₂/Ar) were cooled down from 298 K to 160 K with and without the cooling field of $1.6 \times 10^6 \text{ A/m}$. In the ion-beam bombardment experiment, the (Ni, Co)O (26% O₂/Ar) layers were bombarded by Ar⁺ ion-beam with V_{EH} varied from 0 V to 150 V for 5 min before the deposition of the top NiCo layer. Then, the bilayers were field cooled to 5 K with a magnetic field of $1.6 \times 10^6 \text{ A/m}$.

The crystalline structures of the samples were measured by Rigaku D/MAX2500 X-ray Diffractometer with Cu K α radiation ($\lambda = 0.154 \text{ nm}$). A JEOL Transmission Electron Microscope (JEM-2010) operating at 200 kV was engaged in obtaining the microstructures of the samples. To

make the samples electron-transparent for taking both planar-view and cross-sectional TEM images, the samples were grinded with sand papers and thinned down by a Gatan ion-mill system. Magnetic properties were characterized by an ADE-DMS 1660 Vibrating Sample Magnetometer (VSM) at room temperature and at 160 K under zero-field-cooling (ZFC) or field-cooling (FC) processes from 298 K with applied magnetic field ($H = 1.6 \times 10^6 \text{ A/m}$) parallel to the film plane; and at 5 K under FC processes by Quantum Design MPMS-7 Superconducting Quantum Interference Device (SQUID) magnetometer. Photoemission electron microscopy (PEEM) was conducted in the National Synchrotron Radiation Research Center (NSRRC) in Taiwan to investigate the morphology of domain patterns. VEECO (DI-3100) Atomic/Magnetic Force Microscope (AFM/MFM) operated under tapping mode with a Co-alloy coated tip was utilized to investigate the domain structures at the sample surfaces.

3. Results and discussion

The crystalline structures of (Ni, Co)O single layers prepared with different O₂/Ar ratios can be analyzed from the X-ray diffraction (XRD) patterns (Fig. 1). For the samples prepared with 0% and 8% O₂/Ar, two major peaks emerged at $2\theta = 44^\circ$ and 76° . These two peaks corresponded to the (111) and (220) planes of FCC NiCo, and the calculated lattice constant was 3.53 Å. The lower peaks at $2\theta = 36^\circ$, 62° and 76° , corresponding to the (111), (220) and (311) orientations of (Ni, Co)O respectively, indicated that the content of oxide was relatively low in (Ni, Co)O single layer (8% O₂). However, when the oxygen ratio was increased to 26%, (Ni, Co)O (200) peak and sharp (Ni, Co)O (311) peak could be observed, and the (Ni, Co)O (220) and (111) peaks were also greatly strengthened. By further increasing the oxygen content to 30%, the (Ni, Co)O (311) was weakened, and (111) and (220) remained to be the preferred orientations. The lattice structure of (Ni, Co)O was Rocksalt FCC with lattice constant of 4.29 Å.

As reported previously [18], the changes in composition and preferred orientation resulted from the in-situ oxidization of NiCo. For the samples prepared with low oxygen content (0% and 8%), the major composition of the layers was NiCo. When the oxygen content reached 26%, antiferromagnetic (Ni, Co)O was formed despite the fact that a flat NiCo peak could also be observed at $2\theta = 44^\circ$. This transition in composition resulted in remarkable changes in the magnetic properties of the bilayers. When O₂/Ar ratio was further increased to 30%, the change in the preferred crystalline orientation led to transformation in spin and magnetic structures, which in turn affected the exchange coupling between NiCo and (Ni, Co)O. These phenomena are discussed as follows.

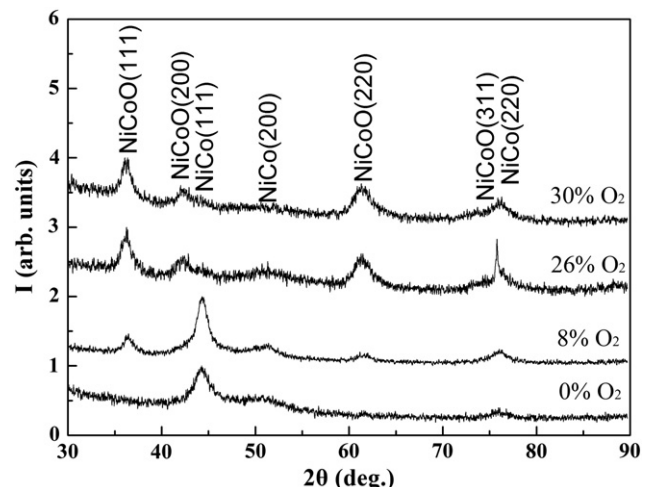


Fig. 1. The grazing angle XRD patterns of (Ni, Co)O (0%, 8%, 26%, and 30% O₂/Ar).

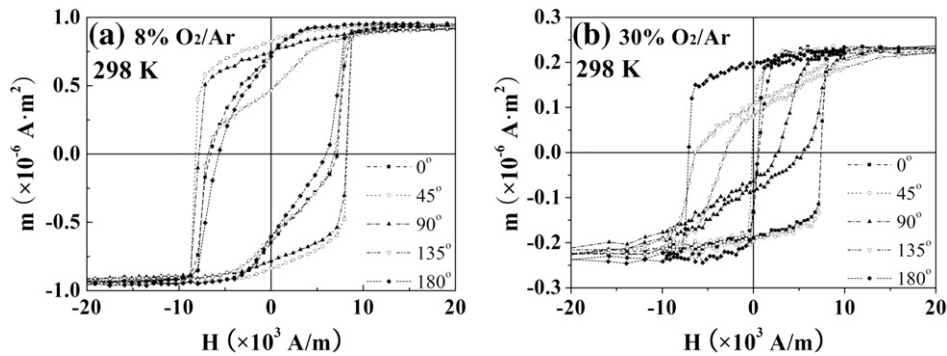


Fig. 2. Hysteresis loops measured at different angles at 298 K for samples (a) NiCo/(Ni, Co)O (8% O₂/Ar) and (b) NiCo/(Ni, Co)O (30% O₂/Ar).

3.1. Cooling field effect and angular dependence of the coercivity and exchange bias of NiCo/(Ni, Co)O

As shown in Fig. 2, the hysteresis loops of NiCo/(Ni, Co)O (8% and 30% O₂/Ar) were measured at 298 K with different in-plane angles. Compared with the H_C of the pure NiCo (~1.6 kA/m at room temperature), the coercivities of the bilayers measured at 0° (6.8 kA/m and 3.4 kA/m) were greatly enhanced, which was believed to be the characteristic of exchange coupling between ferromagnetic NiCo and antiferromagnetic (Ni, Co)O [6]. No evident exchange bias effect was observed in the samples prepared with 8% O₂/Ar (H_{ex} ~ 0.32 kA/m), while NiCo/(Ni, Co)O (30% O₂/Ar) presented large positive H_{ex} (~4.0 kA/m). This distinction could be explained by the different compositions of the two samples. As discussed in the XRD patterns, the content of oxide was relatively low in the bilayers prepared with 8% O₂/Ar. In addition, the antiferromagnetism of (Ni, Co)O is rather weak at room temperature. As a result, the exchange coupling in NiCo/(Ni, Co)O (8% O₂/Ar) was relatively weak, which in turn led to the small H_{ex} (0.32 kA/m). When O₂/Ar ratio reached 30%, the content of (Ni, Co)O increased and the exchange coupling was enhanced, resulting in the larger exchange bias field. The positive H_{ex} is believed to be the result of the antiferromagnetic coupling in the interface [28]. The reduction in square ratios of hysteresis loops in NiCo/(Ni, Co)O (30% O₂/Ar) indicated the change in NiCo anisotropy because of interfacing with the AF (Ni, Co)O.

To further investigate the cooling field effect, the NiCo/(Ni, Co)O (30% O₂/Ar) bilayers were cooled down to 160 K with and without the cooling field of 1.6×10^6 A/m. The hysteresis loops of the samples under ZFC and FC are presented in Fig. 3. When measured at 0°, the ZFC samples exhibited positive H_{ex}, similar to that measured at room temperature. This could be explained by the fact that the exchange coupling between AF and FM layers remained antiferromagnetic in the ZFC process. In addition, since antiferromagnetism of (Ni, Co)O was enhanced at low temperature, the AF coupling was strengthened. As a consequence, H_{ex} (6.3 kA/m) and H_C (35.7 kA/m) were both enlarged. However, after field cooling process, the exchange bias field shifted to

negative (−3.7 kA/m). This indicated that the exchange coupling changed from AF to FM. In the field cooling process, the large applied field not only maintained the single domain state [30] of the FM layer but also altered the orientation of AF spin. As a result, the AF spins canted towards the orientation of the cooling field, leading to FM exchange coupling.

The angular dependence of H_{ex} and H_C at room temperature and 160 K is shown in Fig. 4. The angular dependence of H_C of both bilayers showed some periodicity. The H_C of NiCo/(Ni, Co)O (8% O₂/Ar) bilayers reached minimum at 0°, 180° and 360° (i.e. perpendicular to the easy axis of the FM materials), while ramped to maximum at 90° and 270° (i.e. parallel with the easy axis). The H_C curves of NiCo/(Ni, Co)O (30% O₂/Ar) bilayers exhibited different characteristics. H_C was largest at 0°, 180°, while dropped to the minimum at 90° and 270°. However, one thing in common is that they both demonstrated cosinusoidal relationship with period of 180°. H_{ex} curves of NiCo/(Ni, Co)O (30% O₂/Ar) bilayers also illustrated cosinusoidal traces, which are consistent with the previous theoretical simulations [31,32]. It should be noted that the period for H_{ex} is 360°, twice as large as that for H_C. The H_{ex} measured at 298 K shifted from positive to negative in 135°–270°. Similar angular dependence could be observed at 160 K when the samples were cooled down without magnetic field. However, after field cooling process, H_{ex} remained negative, regardless of measuring angle. This indicated that through field cooling, the sign of exchange bias could be defined. Note that the different values measured at 0° and 360° are considered to be a result of the training effect.

Direct evidence of the surface domain structures could be observed by PEEM as shown in Fig. 5. Large domains were observed in the NiCo alloy (Fig. 5(a)) while entangled long continuous stripe domains appeared on the surface of the NiCo/(Ni, Co)O (8% O₂/Ar) bilayer (Fig. 5(a)). As the bottom layers were further oxidized with higher O₂/Ar ratio, the surface domain patterns changed to short fine stripes (Fig. 5(c) and (d)). From these variations in domain patterns, we could see that the changes in microstructure of the bottom layers resulted in vast changes in the shape and size of the surface magnetic domain patterns, thus modifying the magnetic properties of the bilayers.

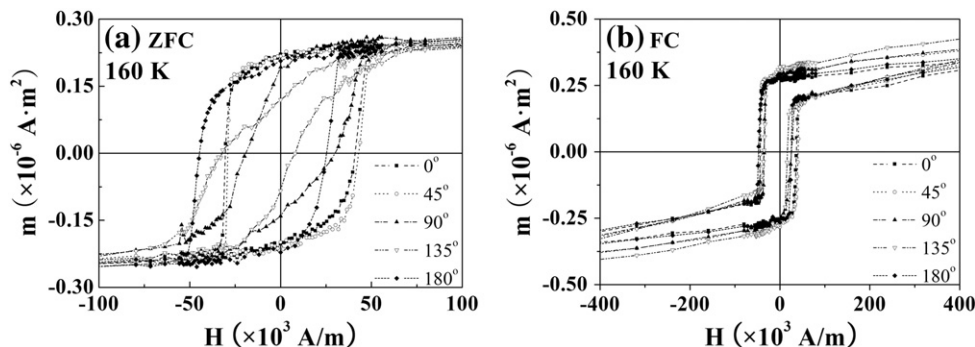


Fig. 3. Hysteresis loops of NiCo/(Ni, Co)O (30% O₂/Ar) measured at different angles at 160 K after (a) the zero field cooling and (b) the field cooling process.

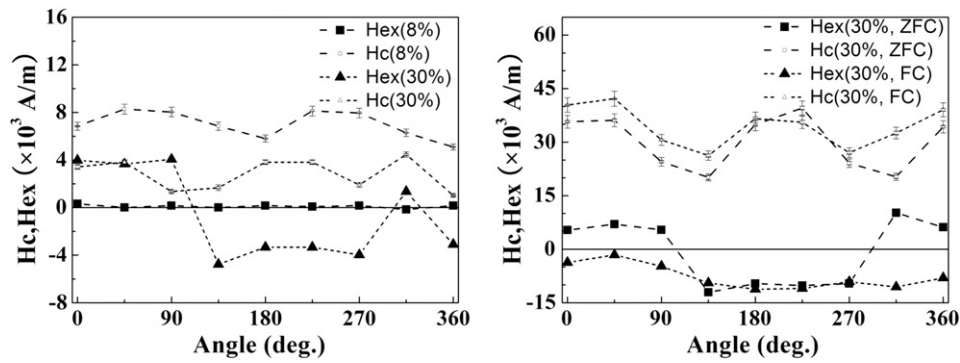


Fig. 4. Angular dependence of H_c and H_{ex} of NiCo/(Ni, Co)O (8% O_2/Ar) and NiCo/(Ni, Co)O (30% O_2/Ar) at 298 K and 160 K.

3.2. Ion-beam bombardment effects

Ar^+ ion-beam bombardment with V_{EH} ranging from 0 V to 150 V was conducted on the surface of (Ni, Co)O (26% O_2/Ar), resulting in remarkable changes in both microstructure and magnetic properties. The surface morphology and cross-sectional profile were characterized by TEM as shown in Fig. 6. A smooth interface between the top NiCo and the bottom (Ni, Co)O layer (thickness variation less than 2 nm) could be seen from the cross-section profile (Fig. 6(a)). This indicated that the layers exhibited low surface roughness and weak diffusion. In the electron diffraction rings (Fig. 6(b)), the corresponding crystal planes of rock-salt FCC (Ni, Co)O ((111), (200), and (220)) and FCC NiCo ((200), (222), and (311)) could be observed. The preferred orientations measured by TEM are in good accordance with the results characterized by XRD. The bright field images show the high resolution surface morphologies of the bilayers bombarded by $V_{EH} = 0$ V (Fig. 6(c)), $V_{EH} = 70$ V (Fig. 6(d)), and $V_{EH} = 130$ V (Fig. 6(e)). The grain sizes of all the

samples ranged from 5 nm to 15 nm, and reached the maximum when V_{EH} was 70 V. Noticeable fold structure was observed on the bilayer bombarded by $V_{EH} = 130$ V (Fig. 6(e)). This indicated that the ion-beam bombardment significantly modified the surface morphology of (Ni, Co)O, and this deformation altered the surface structure of upper NiCo. These changes in microstructure also led to different magnetic properties, which is discussed later.

In order to study the influence of ion-beam bombardment of the (Ni, Co)O surface on the magnetic properties of NiCo/(Ni, Co)O bilayers, the magnetic properties of all the samples were characterized twice, one at 298 K and one after 1.6×10^6 A/m field cooling to 5 K. In Fig. 7, shifted hysteresis loops and enhanced coercivities could be observed in the bilayers at 298 K and at 5 K. This asymmetry in hysteresis loops was a strong evidence for the unidirectional anisotropy provided by the interfacial (Ni, Co)O moments coupled to the NiCo moments. Two mechanisms were responsible for the magnetic reversal process when the bilayers were saturated by the negative magnetic field. The round

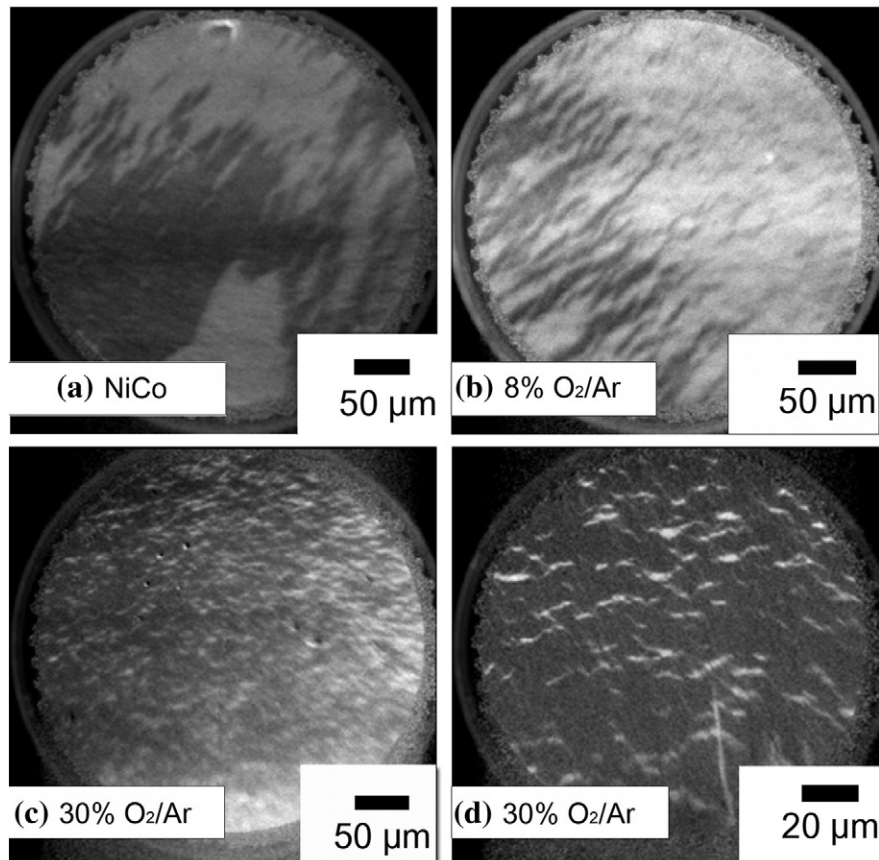


Fig. 5. The magnetic domain patterns by PEEM for (a) NiCo, (b) NiCo/NiCoO (8% O_2/Ar), and (c) and (d) NiCo/NiCoO (30% O_2/Ar).

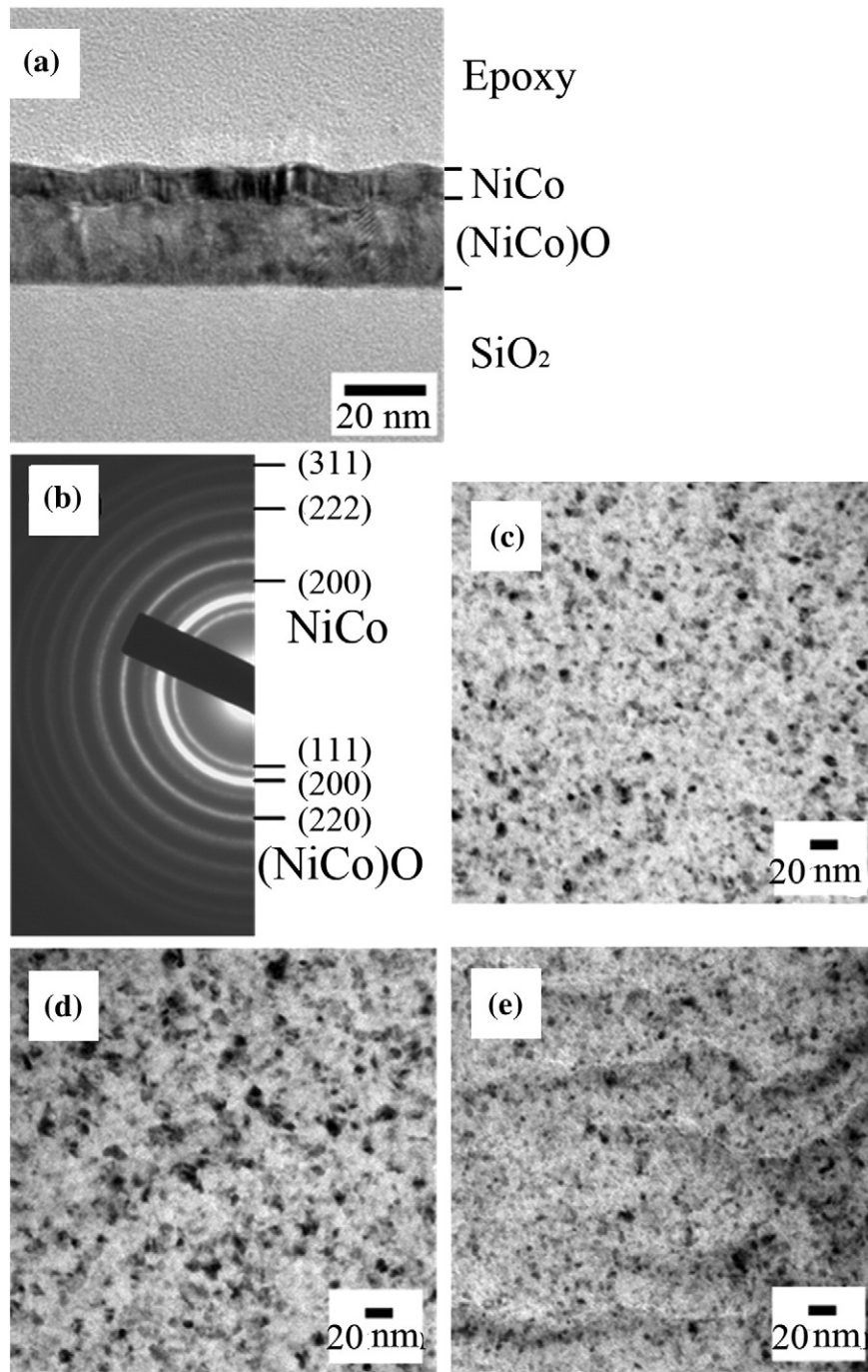


Fig. 6. TEM characterizations of NiCo/(Ni, Co)O bilayers bombarded by various End-Hall voltages: (a) cross-section morphology of $V_{EH} = 70$ V, (b) diffraction pattern of $V_{EH} = 0$ V, and the bright field images of (c) $V_{EH} = 0$ V, (d) $V_{EH} = 70$ V, and (e) $V_{EH} = 130$ V.

hysteresis loops of the NiCo/(Ni, Co)O ($V_{EH} = 0$ V (Fig. 7(a)), 70 V (Fig. 7(b)) and 130 V (Fig. 7(c)) bilayers indicated that the magnetization reversal was likely dominated by the rotation of the interfacial magnetization [33]. However, the hysteresis loop of bilayers bombarded by $V_{EH} = 150$ V (Fig. 7(d)) is more rectangular in shape and exhibited a magnetic reversal process dominated by the domain wall motion [6].

In addition, the hysteresis loops split into two subloops when measured at 298 K, and this phenomena was enhanced when $V_{EH} = 70$ V. Similar complex hysteresis loops were also observed in nanocomposite Co/CoO thin films [7]. Yi et al. attributed the presence of the two subloops to the competition between dipolar interaction and exchange coupling. As discussed in the X-ray diffraction patterns (Fig. 1), a small

content of NiCo existed in the (Ni, Co)O (26% O_2/Ar). The dipolar interaction between the NiCo contents in the bottom and the top layer contributed to positive H_{ex} , while the exchange coupling between (Ni, Co)O and NiCo acted oppositely. After the FC process to 5 K, the exchange coupling between the FM and AF layer was greatly enhanced, and the magnetic performance of the bilayer was dominated by the exchange coupling. As a result, the two subloops merged into one at 5 K. It should be noted that the negative H_{ex} in the NiCo/(Ni, Co)O (26% O_2/Ar , $V_{EH} = 0$ V) indicated a FM exchange, which was different from the coupling mechanism of the NiCo/(Ni, Co)O (30% O_2/Ar). This variation could be due to the different contents and microstructures between the two samples.

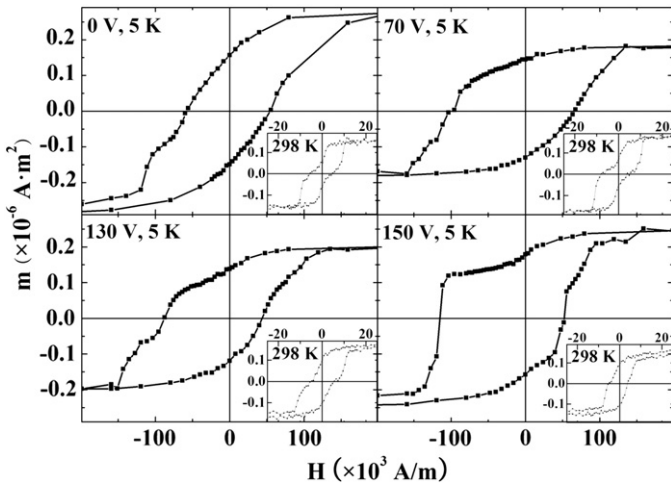


Fig. 7. Hysteresis loops of NiCo/(Ni, Co)O bilayers bombarded by (a) $V_{EH} = 0$ V, (b) $V_{EH} = 70$ V, (c) $V_{EH} = 130$ V, and (d) $V_{EH} = 150$ V measured at 5 K and 298 K (insets).

The variations of H_C and H_{ex} with V_{EH} measured at 298 K and 5 K are plotted in Fig. 8(a) and (b), respectively. At 298 K, the measured H_C changed slightly after ion-beam bombardment process, ranging from 5.1 kA/m to 6.0 kA/m. However, H_{ex} exhibited significant fluctuation. When V_{EH} reached 70 V, the most enhanced H_{ex} (-2.1 kA/m) was observed. However, as the ion-beam energy increased, H_{ex} changed to 80 A/m at $V_{EH} = 130$ V. Further increasing the bombardment voltage to 150 V failed to enhance the positive exchange bias. On the contrary, H_{ex} shifted to -1.6 kA/m as a result of the structural deformation. McCord et al. [34] proved that tilted exchange anisotropy is responsible for the loop asymmetry in exchange-coupled FM/AF thin films. The influence of ion-beam bombardment on the AF surface is twofold [33]. On one hand, the bombardment alters the tilted FM/AF exchange unidirectional anisotropy. The misalignment between this exchange anisotropy and FM uniaxial anisotropy leads to declined exchange coupling strength and reduced H_{ex} . On the other hand, uncompensated interfacial spins are created as a result of the structural deformation, which may enhance the exchange bias effect. In the case of moderate Ar^+ ion-beam bombardment ($V_{EH} = 70$ V), the largest H_{ex} (-2.1 kA/m) was likely due to the uncompensated AF spins which was created during the ion-beam bombardment process. As the ion energy increased, tilted spins emerged and resulted in misaligned interfacial spins. This in turn led to declined exchange coupling strength and reduced H_{ex} .

After the FC process to 5 K, a different dependence pattern on V_{EH} was observed in the H_C and H_{ex} . With increasing V_{EH} , the exchange bias was greatly enhanced, and H_{ex} reached maximum at $V_{EH} = 150$ V (-31.5 kA/m). As a consequence of the enhanced exchange coupling effect, H_C also increased greatly after the ion-beam bombardment

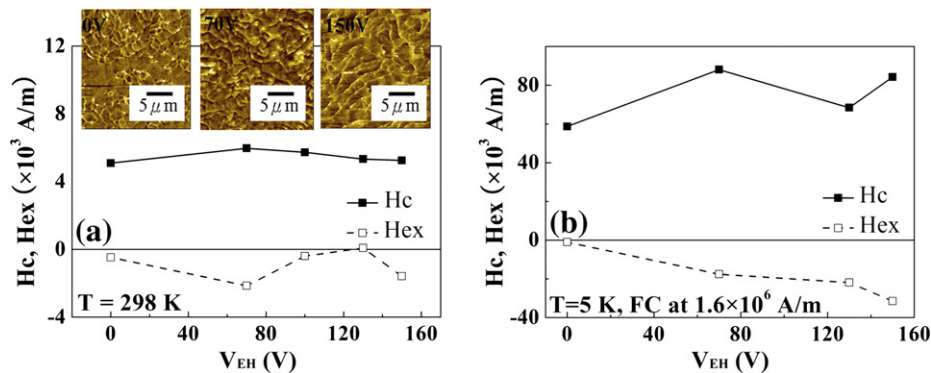


Fig. 8. Dependence of H_C and H_{ex} on V_{EH} for NiCo/(Ni, Co)O bilayers measured at (a): 298 K and (b): 5 K after the field cooling process, and (a) inset: domain patterns at 298 K measured by MFM.

process. The cooling field effect was responsible for the enhanced H_{ex} at 5 K. As discussed above, the FC process affected the bilayers by aligning the AF spins towards the cooling field orientation. As a result, the misalignment between the interfacial moments and the exchange anisotropy was reduced. The reduction in misalignment and the increase in uncompensated interface spins resulted in the enhanced exchange coupling with increased ion-beam energies. After ion-beam bombardment of $V_{EH} = 150$ V, the interfacial exchange energy density calculated from Eq. (1) was 3.1×10^{-4} J/m².

The ion-beam bombardment on the bottom layer also resulted in obvious changes in surface domain patterns (Fig. 8 inset). As V_{EH} increased, the domains elongated to stripes of around 1 μ m in width. These changes indicated that the initial FM domain states are strongly affected by interfacing with the different ion-beam bombarded AF layers during the magnetization reversal process. These results are consistent with our previous research on NiFe/Mn [33] and NiFe/(Ni, Fe)O [26] bilayers.

4. Conclusions

NiCo/(Ni, Co)O bilayers were prepared by dual-ion-beam-deposition technique with O_2/Ar ratio ranging from 0% to 30%, and the microstructure and magnetic properties were investigated. The bilayers consisted of FCC NiCo (3.53 Å) and rock-salt (Ni, Co)O (4.29 Å), as characterized by XRD and TEM. The cooling field effect and angular dependence of the coercivity and exchange bias field was analyzed at room temperature and 160 K. For the samples measured at 298 K, H_{ex} switched from positive to negative as the measuring angle changed from 0° to 135°. After the ZFC process, similar angular dependence was observed. The H_{ex} of the field cooled samples remained negative at different angles, indicating the existence of FM coupling. Such transition proved that FC process could dictate the exchange coupling mechanism. The Ar^+ ion-beam bombardment could create uncompensated AF spins (enhancing H_{ex}) and increase spin misalignment in the interface (diminishing H_{ex}). At 298 K, strongest exchange coupling was exhibited as a result of moderate ion bombardment. After FC process, enhancement of H_{ex} with increasing ion energy was observed, indicating that the exchange bias was contributed by the uncompensated interface spins. This work demonstrated that the polarity of exchange bias can be adjusted by the cooling field process, angular dependence of magnetic properties, and ion-beam bombardment. These results provided feasible means to tailor the magnetic properties of magnetic thin films, which could be applied in spintronic devices such as exchange biased giant magnetoresistance sensors and magnetic tunnel junctions. Further study will be conducted to establish the theoretical model in order to explain and predict the modifications in magnetic properties by engaging the techniques developed in this work. Moreover, further experiments will be carried out to reveal the influence of thin-film geometry and post-annealing on the exchange bias of (Ni, Co)O bilayers.

References

- [1] W.H. Meiklejohn, C.P. Bean, New magnetic anisotropy, *Phys. Rev.* 105 (1957) 904.
- [2] S. Giri, M. Patra, S. Majumdar, Exchange bias effect in alloys and compounds, *J. Phys. Condens. Matter* 23 (2011) (073201).
- [3] M. Patra, M. Thakur, S. Majumdar, S. Giri, The exchange bias effect in phase separated $\text{Nd}_{1-x}\text{Sr}_x\text{CoO}_3$ at the spontaneous ferromagnetic/ferrimagnetic interface, *J. Phys. Condens. Matter* 21 (2009) (236004).
- [4] F. Radu, R. Abrudan, I. Radu, D. Schmitz, H. Zabel, Perpendicular exchange bias in ferrimagnetic spin valves, *Nat. Commun.* 3 (2012) 715.
- [5] F. Radu, S.K. Mishra, I. Zizak, A.I. Erko, H.A. Dürr, W. Eberhardt, G. Nowak, S. Buschhorn, H. Zabel, K. Zhernenkov, M. Wolff, D. Schmitz, E. Schierle, E. Dudzik, R. Feyerherm, Origin of the reduced exchange bias in an epitaxial $\text{FeNi}(111)/\text{CoO}(111)$ bilayer, *Phys. Rev. B* 79 (2009) 184425.
- [6] A.E. Berkowitz, K. Takano, Exchange anisotropy – a review, *J. Magn. Magn. Mater.* 200 (1999) 552.
- [7] J.B. Yi, J. Ding, B.H. Liu, Z.L. Dong, T. White, Y. Liu, Exchange bias and magnetization process of Co/CoO nanocomposite thin films, *J. Magn. Magn. Mater.* 285 (2005) 224.
- [8] J. Nogués, D. Lederman, T.J. Moran, I.K. Schuller, Positive exchange bias in FeF_2 – Fe bilayers, *Phys. Rev. Lett.* 76 (1996) 4624.
- [9] M. Kiwi, J. Mejía-López, R.D. Portugal, R. Ramírez, Positive exchange bias model: Fe/FeF_2 and Fe/MnF_2 bilayers, *Solid State Commun.* 116 (2000) 315.
- [10] J. Nogués, C. Leighton, I.K. Schuller, Correlation between antiferromagnetic interface coupling and positive exchange bias, *Phys. Rev. B* 61 (2000) 1315.
- [11] K.W. Lin, Y.M. Tzeng, Z.Y. Guo, C.Y. Liu, J. van Lierop, Positive exchange bias in a $\text{Ni}_{80}\text{Fe}_{20}/\text{Ni}_x\text{Fe}_{1-x}\text{O}$ thin-film bilayer, *J. Magn. Magn. Mater.* 304 (2006) e124.
- [12] D.Z. Yang, J. Du, L. Sun, X.S. Wu, X.X. Zhang, S.M. Zhou, Positive exchange biasing in GdFe/NiCoO bilayers with antiferromagnetic coupling, *Phys. Rev. B* 71 (2005) 144417.
- [13] B. Altunçevahir, A.R. Koymen, Positive and negative exchange bias in $\text{CoNi}/\text{Gd}/\text{CoNi}$ trilayers and CoNi/Gd bilayers, *J. Magn. Magn. Mater.* 261 (2003) 424.
- [14] M.J. Pechan, D. Bennett, N.C. Teng, C. Leighton, J. Nogués, I.K. Schuller, Induced anisotropy and positive exchange bias: a temperature, angular, and cooling field study by ferromagnetic resonance, *Phys. Rev. B* 65 (2002) (064410-064411-064415).
- [15] N.C. Koon, Calculations of exchange bias in thin films with ferromagnetic/antiferromagnetic interfaces, *Phys. Rev. Lett.* 78 (1997) 4865.
- [16] R. Jungblut, R. Coehoorn, M.T. Johnson, J.a. de Stegge, A. Reinders, Orientational dependence of the exchange biasing in molecular-beam-epitaxy-grown $\text{Ni}_{80}\text{Fe}_{20}/\text{Fe}_{50}\text{Mn}_{50}$ bilayers (invited), *J. Appl. Phys.* 75 (1994) 6659.
- [17] K.W. Lin, R.J. Gambino, L.H. Lewis, Structural and magnetic characterization of ion-beam deposited $\text{NiFe}/\text{Ni}_x\text{Fe}_{1-x}\text{O}$ composite films, *J. Appl. Phys.* 93 (2003) 6590.
- [18] K.W. Lin, J.Y. Guo, H.Y. Liu, H. Ouyang, Y.L. Chan, D.H. Wei, J. van Lierop, Anomalous exchange bias behavior in ion-beam bombarded $\text{NiCo}/(\text{Ni},\text{Co})\text{O}$ bilayers, *J. Appl. Phys.* 103 (2008) (07C105-103).
- [19] S. Mangin, F. Montaigne, A. Schuhl, Interface domain wall and exchange bias phenomena in ferrimagnetic/ferrimagnetic bilayers, *Phys. Rev. B* 68 (2003) 140404.
- [20] F. Canet, C. Bellouard, S. Mangin, C. Chatelain, C. Senet, R. Siebrecht, V. Leiner, M. Piecuch, Exchange bias like effect induced by domain walls in FeGd/FeSn bilayers, *Eur. Phys. J. B* 34 (2003) 381.
- [21] T.L. Kirk, O. Hellwig, E.E. Fullerton, Coercivity mechanisms in positive exchange-biased Co films and Co/Pt multilayers, *Phys. Rev. B* 65 (2002) 224426.
- [22] R. Jungblut, R. Coehoorn, M.T. Johnson, J.a. de Stegge, A. Reinders, Orientational dependence of the exchange biasing in molecular-beam-epitaxy-grown $\text{Ni}[\text{sub } 80] \text{Fe}[\text{sub } 20]/\text{Fe}[\text{sub } 50]\text{Mn}[\text{sub } 50]$ bilayers, *J. Appl. Phys.* 75 (1994) 6659.
- [23] K.W. Lin, M. Mirza, C. Shueh, H.R. Huang, H.F. Hsu, J. van Lierop, Tailoring interfacial exchange coupling with low-energy ion beam bombardment: tuning the interface roughness, *Appl. Phys. Lett.* 100 (2012) 122409.
- [24] J. Fassbender, D. Ravelosona, Y. Samson, Tailoring magnetism by light-ion irradiation and implantation, *J. Phys. D: Appl. Phys.* 37 (2004) R179.
- [25] J. Fassbender, J. McCord, Magnetic patterning by means of ion irradiation and implantation, *J. Magn. Magn. Mater.* 320 (2008) 579.
- [26] K.W. Lin, M.R. Wei, J.Y. Guo, Cooling field and ion-beam bombardment effects on exchange bias behavior in $\text{NiFe}/(\text{Ni},\text{Fe})\text{O}$ bilayers, *J. Nanosci. Nanotechnol.* 9 (2009) 2023.
- [27] G. Li, C.W. Leung, C. Shueh, H.-F. Hsu, H.-R. Huang, K.-W. Lin, P.T. Lai, P.W.T. Pong, Exchange bias effects of NiFe/NiO bilayers through ion-beam bombardment on the NiO surface, *Surf. Coat. Technol.* 228 (2013) S437.
- [28] H. Ouyang, K.W. Lin, C.C. Liu, S.-C. Lo, Y.M. Tzeng, Z.Y. Guo, J. van Lierop, Exchange bias dependence on interface spin alignment in a $\text{Ni}_{80}\text{Fe}_{20}/(\text{Ni},\text{Fe})\text{O}$ Thin Film, *Phys. Rev. Lett.* 98 (2007) 097204.
- [29] K.W. Lin, P.H. Ko, Z.Y. Guo, H. Ouyang, J. van Lierop, Tuning the exchange bias in NiFe/Fe -oxide bilayers by way of different Fe-oxide based mixtures made with an ion-beam deposition technique, *J. Nanosci. Nanotechnol.* 7 (2007) 265.
- [30] P. Miltényi, M. Gierlings, M. Bammig, U. May, G. Güntherodt, J. Nogués, M. Gruyters, C. Leighton, I.K. Schuller, Tuning exchange bias, *Appl. Phys. Lett.* 75 (1999) 2304.
- [31] J.-V. Kim, R.L. Stamps, B.V. McGrath, R.E. Camley, Angular dependence and interfacial roughness in exchange-biased ferromagnetic/antiferromagnetic bilayers, *Phys. Rev. B* 61 (2000) 8888.
- [32] M.D. Stiles, R.D. McMichael, Coercivity in exchange-bias bilayers, *Phys. Rev. B* 63 (2001) 064405.
- [33] K.W. Lin, T.J. Chen, J.Y. Guo, H. Ouyang, D.H. Wei, J. Van Lierop, Correlating antiferromagnetic spin structures with ion-beam bombardment in exchange-biased NiFe/Mn bilayers, *J. Appl. Phys.* 105 (2009) (07D710-707D710-713).
- [34] J. McCord, C. Hamann, R. Schäfer, L. Schultz, R. Mattheis, Nonlinear exchange coupling and magnetic domain asymmetry in ferromagnetic/IrMn thin films, *Phys. Rev. B* 78 (2008) 094419.